Perpendicular wavenumber dependence of $E \times B$ flows on the linear stability of global ITG modes

P. Hill[1,2], S. Saarelma[2], E. Verwichte[1]

[1] *CFSA, University of Warwick, Coventry, UK*

[2] *EURATOM/CCFE Association, Culham Science Centre, Abingdon, Oxon, OX14 3DB, UK.*

It is well-known that sheared flows (whether the so-called "intrinsic" rotation[1, 2], self-generated by turbulence[3], or driven by external means such as NBI[4]) can suppress turbulence [3, 5] or even stabilise the underlying linear mode driving the turbulence[3, 6]. This suppression has been well studied in the limit when the normalised gyro-radius $\rho_* = \rho_i/a$ becomes vanishingly small, in both slab and toroidal geometries. In the $\rho_* \to 0$ ("local") limit profile variations are neglected. Local codes often have a simulation domain on the order of hundreds of ρ_i. However, spherical tokamaks, such as MAST, have a small aspect-ratio and operate with finite ρ_* ($\sim 1/50$). The flows in spherical tokamaks can also approach the sonic speed. The combination of these effects means that it is necessary to use global numerical codes which simulate the full 3D domain.

Sheared flows stabilise linear modes by convecting the mode structure in the ballooning angle[7], rotating from the outboard, "bad curvature" side to the inboard, "good curvature" side. Because a rotating mode samples the good curvature region, its growth rate is necessarily smaller than one whose ballooning angle stays fixed on the outboard side. Another way to think of this is that the flow shear tilts the mode structure

Linear instabilies are stabilised when the shearing rate, γ_E, reaches some critical value, γ_E^{crit}, roughly equal to the growth rate of the mode without flow, γ_0. Numerous simulations[5] have found $0.4 \lesssim \gamma_E^{crit}/\gamma_0 \lesssim 2$. This current work investigates how the magnitude of the suppression from sheared flows changes with $k_\perp$ in ion-temperature-gradient-driven (ITG) modes in the MAST tokamak. We also present some early results from non-linear simulations.

MAST equilibrium with experimental rotation profile

We use equilibrium profiles reconstructed from TRANSP (Fig. 1). The radial electric field is calculated from the toroidal angular frequency profile and a canonical Maxwellian is used to provide a parallel velocity profile. Figure 1 shows the calculated linear growth rate spectrum with and without flow. With the experimental rotation profile, the linear modes are almost completely stabilised, with only some long wavelength modes surviving (though their growth rates are small, $\gamma \lesssim 0.01 v_{th}/a$).

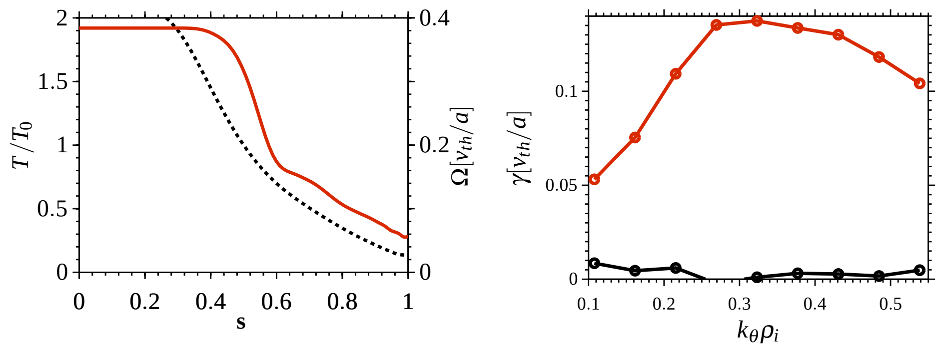

Figure 1: Left: Angular frequency rotation (red, solid) and temperature (black, dashed) profiles for MAST shot #22807. The radial coordinate is $s = \sqrt{\psi/\psi_{\rm edge}}$ and the temperature is normalised to its value at $s = 0.5$. Right: Calculated linear growth rate spectrum with (red line) and without (black line) experimental rotation profile

We perform a scan in γ_E by scaling the rotation profile in Fig. 1 and calculating the average shearing rate in the region where the linear mode sits. Negative shearing rates correspond to rotation in the experimental direction (co-current), with counter-current rotation having positive shearing rates. Figure 3 shows the asymmetry with respect to shear direction for the fastest growing mode, $k_\theta \rho_i = 0.32$, and a long wavelength mode, $k_\theta \rho_i = 0.11$. The maximum growth rate occurs at $\gamma_E = 0.0624$, 10% of the experimental level. This asymmetry is caused by the equilibrium profiles (temperature, density) varying over the length scale of the instability, changing its local mode frequency[6]. This shear in the frequency acts in a similar way to flow shear (Fig. 2), tilting the mode, reducing its linear growth rate. Flow shear in one direction then has to “un-tilt” the mode before it can stabilise it, whereas shear in the opposite direction can start stabilising the mode straight away. Because this effect is caused by profile variation, local models do not capture it. This is a clear example where a global code which retains all the profile variation effects is required to capture the suppression asymmetry.

While the fastest growing linear mode is stabilised as expected, with $\gamma_E^{crit}/\gamma_0 \sim 2$ (Fig. 3), longer wavelength modes can have $\gamma_E^{crit}/\gamma_0 > 6$. This is surprising as [6] says that γ_E^{crit}/γ_0 should go as $k_\theta \rho_i$. This can be understood in an intuitive picture — larger structures would be more affected by the flow shear and so by stabilised faster. It seems to be the case that actually both longer and shorter wavelengths are stabilised quicker than the fastest growing mode.

MAST equilibrium with experimental rotation profile and kinetic trapped electrons

We now include the effects of kinetic trapped electrons while still treating the passing electrons adiabatically. The trapped electrons couple to the ITG modes, enhancing their growth rates without flow by a factor of 4 or more compared to the cases with just adiabatic electrons. Figure

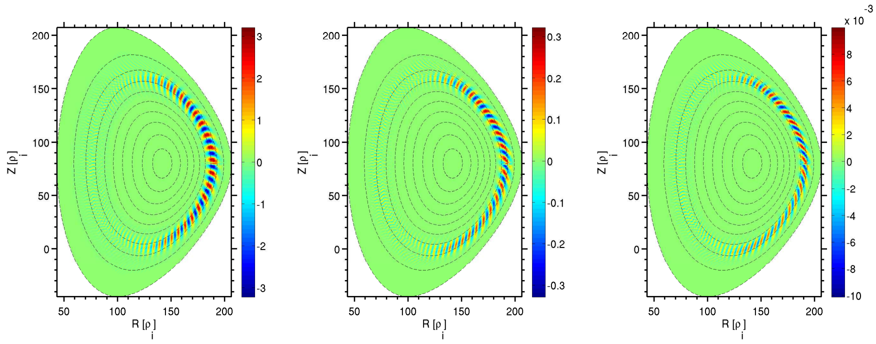

Figure 2: Poloidal cross-section of the perturbed electrostatic potential for different shearing rates. Left to right: $\gamma_E = -0.064$, $\gamma_E = 0.00$, $\gamma_E = 0.064$ (Experimental level $\gamma_E = 0.64$)

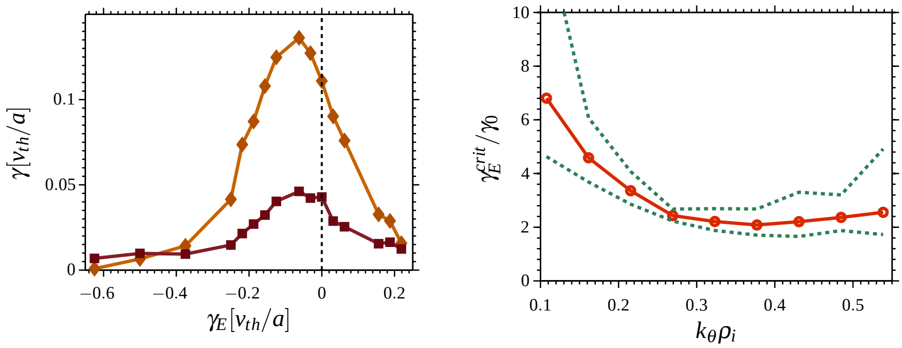

Figure 3: Left: Asymmetry with respect to shear direction for the fastest growing mode (orange diamonds, $k_\theta \rho_i = 0.32$) and a long wavelength mode (red squares, $k_\theta \rho_i = 0.11$). Right: γ_E^{crit}/γ_0 dependence on $k_\theta \rho_i$.

4 shows the $k_\theta \rho_i$ spectrum of growth-rates for rotation in the co- and counter-current directions. Even with flow, the modes are now quite unstable, above the level of the ITG with adiabatic electrons. There is still an asymmetry in the direction of the shear, with counter-current rotation decreasing the growth-rates to less than two-thirds of the growth rates with co-current rotation. The peak of the spectrum also shifts to longer wavelengths with increasing shear in the counter-current direction.

Figure 4 also shows the non-linear heat fluxes. The turbulence spreads inwards from where the linear mode is unstable ($s \sim 0.8$). Including the toroidal rotation strongly reduces the heat flux, as expected, and stops it moving further in than $s \sim 0.4$, where there is a strong gradient in the rotation profile. The difference between the heat fluxes for counter- and co-current rotation is not as great as the difference between the linear growth rates for the two cases. This is because the turbulence also transports perturbed velocity, which can cancel the equilibrium rotation, reducing the shear.

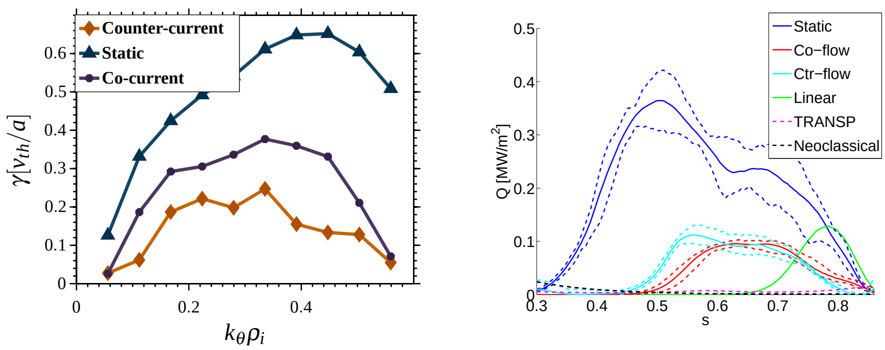

Figure 4: Left: Growth rate spectrum with the inclusion of kinetic electrons for different shearing rates. Right: Non-linear heat fluxes for static and flow cases. The linear flux is included to indicate the position of the linear instability only.

Acknowledgements

This work was funded partly by the RCUK Energy Programme under grant EP/I501045 and the European Communities under the contract of Association between EURATOM and CCFE. The views and opinions expressed herein do not necessarily reflect those of the European Commission. This work was also funded by EPSRC and some simulations were performed using the HPC-FF resource at the Jülich Supercomputing Centre. Other simulations were performed using the HECToR under EPSRC grant EP/H002081.

References

[1] J. E. Rice, Journal of Physics: Conference Series **123**, 012003 (2008).

[2] O. D. GuÌĹrcan, P. H. Diamond, T. S. Hahm, and R. Singh, Physics of Plasmas **14**, 042306 (2007).

[3] P. Terry, Reviews of Modern Physics **72**, 109 (2000).

[4] H. Meyer et al., Nuclear Fusion **49**, 104017 (2009).

[5] K. H. Burrell, Physics of Plasmas **4**, 1499 (1997).

[6] Y. Kishimoto et al., Plasma Physics and Controlled Fusion **41**, A663 (1999).

[7] R. E. Waltz, R. L. Dewar, and X. Garbet, Physics of Plasmas **5**, 1784 (1998).